Ocean Engineering 147 (2018) 243–255

Contents lists available at ScienceDirect

Ocean Engineering

journal homepage: www.elsevier.com/locate/oceaneng

Assessing the size of a twin-cylinder wave energy converter designed for real sea-states

Dali Xu [1], Raphael Stuhlmeier [2], Michael Stiassnie [*]

Faculty of Civil and Environmental Engineering, Technion-Israel Institute of Technology, 32000 Haifa, Israel

ARTICLE INFO

Keywords:
Wave energy
Survivability
Floating cylinders
Broad spectra
Deep water

ABSTRACT

We discuss the hydrodynamics of a wave energy converter consisting of two vertically floating, coaxial cylinders connected by dampers and allowed to heave, surge and pitch. This design, viable in deep water and able to extract energy independent of the incident wave direction, is examined for monochromatic waves as well as broad-banded seas described by a Pierson Moskowitz spectrum. Several possible device sizes are considered, and their performance is investigated for a design spectrum, as well as for more severe sea states, with a view towards survivability of the converters. In terms of device motions and captured power, a quantitative assessment of converter design as it relates to survival and operation is provided. Most results are given in dimensionless form to allow for a wide range of applications.

1. Introduction

The intention of this study is two-fold, providing on one hand a comprehensive account of the hydrodynamics of a system of two coaxial, vertically–floating cylinders envisioned as a model for a wave energy converter (WEC), and subsequently assessing the size and survivability of this system for various sea–states. The optimal size of a floating–body WEC will depend significantly on the length of the waves typically encountered. This dependence highlights a major difficulty of floating-body WEC design: the WEC must be small enough to undergo significant motions, and so generate power, and yet large enough to be robust and survive the challenges of the marine environment.

The system proposed here to model a WEC relies on the relative motion of two bodies, rather than on the motion of a body relative to a fixed frame (which may be either the sea bed or a bottom fixed structure), and is termed a *wave-activated body* or *self-reacting device*. Such devices may be installed in deep water, where the large distance between the sea-bed and the surface would otherwise be prohibitive. The mooring system for such devices has the sole role of counteracting drift and current forces, allowing the weight of moorings and anchors to be relatively small (see (Cerveira et al., 2013) and references therein).

Due to their ubiquity in ocean engineering, a rich literature exists on the interaction of water waves and cylindrical bodies. The radiation problem in heave only was addressed by Ursell (1949), and the scattering problem by Dean and Ursell (1959). Miles and Gilbert (1968) later employed a variational approximation to provide the far field potential for scattering by a circular dock, along with the lateral forces on the dock. However, their results were subsequently found to contain several inaccuracies, in particular in their calculations of the radiation forces. This prompted Garrett (1971) to take up the problem afresh, and establish the scattering forces for a circular dock. Subsequently, Black et al. (1971) revisited the application of variational methods to the radiation and scattering problem by several cylindrical geometries, employing Haskind's theorem to give the wave forces. This latter, variational approach did not yield the added mass and damping coefficients. Hence, some years later Yeung (1981) studied the radiation problem of a vertical cylinder floating on the water surface and undergoing the combined motions of heave, surge and pitch, and obtained these hydrodynamic coefficients. More recently, Bhatta (2007) also gave the added mass and damping coefficient of a vertical cylinder undergoing heave motion, in terms of the two dimensionless ratios characterizing the problem (depth to radius and draft to radius). While prior work had focused on the finite depth case, recently Finnegan et al. (2013) treated by means of an analytical approximation due to Leppington the forces on a truncated vertical cylinder in water of infinite depth.

In the context of wave energy, the consideration of floating cylinders as models of WECs goes back at least to Berggren and Johansson (1992), who approximated a device described by Hagerman by two floating,

* Corresponding author.
E-mail addresses: xudl@shmtu.edu.cn (D. Xu), raphael.stuhlmeier@plymouth.ac.uk (R. Stuhlmeier), miky@technion.ac.il (M. Stiassnie).
[1] Present Address: College of Ocean Science and Engineering, Shanghai Maritime University, 1550 Hai Gang Da Dao, 201306 Shanghai, China.
[2] Present Address: Centre for Mathematical Sciences, Plymouth University, Plymouth, Devon PL4 8AA, United Kingdom.

https://doi.org/10.1016/j.oceaneng.2017.10.012
Received 6 November 2016; Received in revised form 22 August 2017; Accepted 11 October 2017

axisymmetric cylinders oscillating in heave, albeit without any considerations of captured power. More recently, Garnaud and Mei (2010) revisited the single buoy with the intention of studying it in densely packed arrays, giving the captured power for buoys hanging from a large frame. Such a floating, single-cylinder absorber was also employed by Child and Venugopal (2010) in their discussion of optimization of WEC arrays, by Borgarino et al. (2012) as a generic model to investigate wave interaction effects, and many others. Similarly, Teillant et al. (2012) employ an axisymmetric, heaving two-body device for their study of WEC economics, without detailed hydrodynamic considerations. A slightly different fixed–reference WEC was considered by Engström et al. (2009), who added a sphere under the floating cylinder. This two-body configuration of floating cylinder and submerged sphere was then assumed connected to the sea bed by a generator, and its performance analyzed. Zheng et al. (2005), in a generalization of Berggren & Johansson to three modes of motion, considered the hydrodynamics of two unconnected, coaxial floating cylinders, again without considering power capture. The power capture for a self-reacting device consisting of two vertical cylinders moving in heave was recently obtained for attacking monochromatic incident waves by Wu et al. (2014), albeit with a rather terse discussion of their results. Such self-reacting twin cylinder WEC models have the advantage of being feasible in deep water, where reaction against the fixed sea-bed is impractical, while nevertheless allowing for a closed form solution of the linear wave-structure interaction problem, albeit in series form. The submerged lower body can be demonstrated to present a very stable reference to react against, with the performance of such a two-body WEC matching that of a single bottom-referenced cylinder.

The present work combines features of several previous studies, and considers the novel case of two floating cylinders, each allowed to move in all three modes of motion available to an axisymmetric body, connected by an idealized power take–off (PTO) represented by a linear damper of constant characteristics.[3] Subsequent to a detailed description of the wave–structure interaction problem, based on eigenfunction expansion techniques, two main parameters characterizing the device size and damping coefficient are examined. The performance of WECs of different sizes, in terms of explicit values for the motions and captured power, is then given from solutions of the governing equations for various incident waves.

We undertake our parametric study with an eye towards applications, and thus also consider irregular waves in the form of a Pierson-Moskowitz (PM) spectrum (see e.g. recent work on optimizing a floating box-barge under irregular waves by Bódai and Srinil (2015)). While scatter diagrams may be available for some sites where an assessment of the wave resource has been carried out, where this is not the case estimates based on wind speed will need to be made. To this end, we present our data nondimensionalized on the basis of wind speed, which uniquely determines the PM spectrum. Values of significant wave height and peak period may be readily derived therefrom, and the data recast in these terms if desired.

When an incident spectrum is considered, it is no longer possible to assign a simple value to the displacement in heave, surge, and pitch of a floating body. To remedy this, the notion of *significant displacement*, derived from the spectral description of the sea surface, is introduced to give some quantitative information about the three motions of the device. This also allows for a measure of survivability for various WEC sizes and sea-states, by examining under which conditions the device displacements grow large in a statistical sense. An illustrative grading system is devised to categorize the various performance metrics of the self-reacting WECs.

The paper is organized as follows: in Section 2 we present the physical set-up of the problem. This consists in presenting the twin cylinder WEC and characterizing its geometry, and subsequently presenting the PM spectra for design and survivability considerations. In Section 3 we present, very briefly, the basic mathematical formulation of the governing equations and sketch the solution procedure. Subsequently, we employ the hydrodynamic coefficients and forces found from solving the equations of Section 3 to characterizing WEC design under monochromatic waves in Section 4, and under irregular waves given by a Pierson-Moskowitz spectrum in Section 5. A discussion of these results with a view to applications is given in Section 6, which is subdivided into discussions of power capture, survivability, and a brief synthesis of the preceding sections. Finally, Section 7 presents some concluding remarks and perspectives.

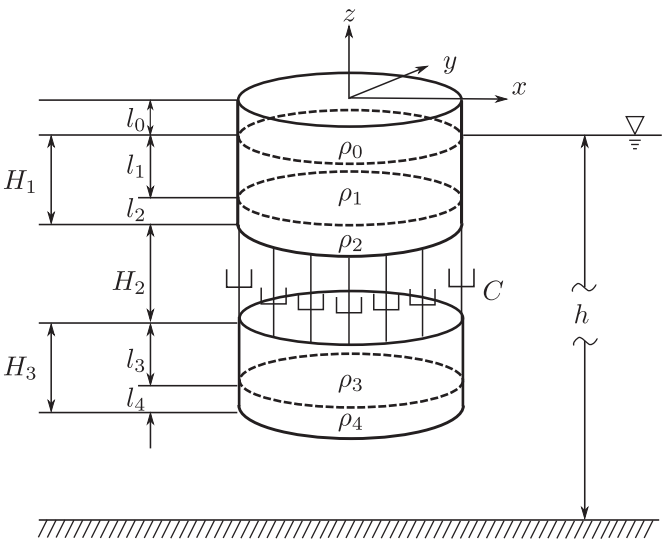

Fig. 1. Schematic depiction of the WEC geometry.

2. Physical preliminaries

2.1. Geometry

The geometry and basic parameters of the twin-cylinder WEC are depicted in Fig. 1. The *Oxy* plane is the still water surface and the *z*-axis points upwards. (r,θ) are polar coordinates in the horizontal plane, such that $x = r\cos\theta$ and $y = r\sin\theta$. The upper cylinder floats on the water surface with a draft H_1. To provide for flotational stability, it is important to note that the mass of this cylinder is not uniformly distributed, but is divided into three parts: a freeboard, i.e. the extension of the cylinder above the wave run-up with height l_0 and density ρ_0, as well as submerged sections with heights l_1 and l_2 and densities ρ_1 and ρ_2, respectively. The lower cylinder is entirely submerged with a height H_3, and assumed to be divided into two parts with densities ρ_3 and ρ_4 and lengths l_3 and l_4, respectively. The distance between the two cylinders in equilibrium is H_2. Both of them have the same radius R, and the water depth h is taken to be very large compared to the attacking wave length, with the intention of approximating deep-water conditions.

As shown in Fig. 1, the two cylinders are connected by a continuously distributed dashpot, which connects the upper edge of the lower cylinder with the lower edge of the upper cylinder at $r = R$. The integrated dashpot coefficient is C, which results in a dashpot coefficient per length $\frac{C}{2\pi R}$. The dashpot is considered to represent a PTO, which generates energy from both the relative heave and pitch motion of the cylinders.[4]

[3] While studies on PTO control show a promising potential for enhancing performance, particularly for devices with a narrow-banded natural response, practical and robust applications must still be developed (see Hong et al. (2014)).

[4] Although the surge motion itself is of first order, the take-off due to sway is a second order quantity, and thus negligible in comparison with the take-off in heave or pitch modes, which are first order.

Since the two cylinders are axisymmetric, only these three modes are studied. The heave and surge motions will give rise to relative motions in z and x directions, respectively. For waves propagating in the $x-$direction, the two cylinders pitch around the y-axis in the mean free surface ($z = 0$), yielding a relative angle about this axis.

This formulation of the problem leaves us with thirteen parameters $(\{H_i | i \in \{1,2,3\}\},\ \{l_j | j \in \{0,1,3\}\},\ \{\rho_j | j \in \{0,1,2,3,4\}\}, R,$ and $C)$ characterizing the WEC. Before proceeding, we will make several restrictions to ensure that the problem remains manageable; nevertheless, we shall see that a wealth of interesting phenomena and properties of the WEC are still accounted for.

For simplicity, we will assume the height of each cylinder, as well as the spacing between the cylinders is identical to their radius, and denote the single size parameter by q, i.e.

$$H_1 = H_2 = H_3 = R \equiv q. \tag{1}$$

For the density distribution of the cylinders, we shall assume

$$\rho_1 = \rho_3 = \frac{3}{4}\rho,\ \rho_2 = \rho_4 = \frac{3}{2}\rho,\ l_1 = l_3 = 2l_2 = 2l_4 = \frac{2}{3}q, \tag{2}$$

where ρ is the density of the water. In order to further reduce the number of parameters we shall choose $\rho_0 \ll \rho$. Thus, the design problem is reduced to two parameters, a size q and dashpot coefficient C, whose interplay with incoming waves of certain frequencies is the issue at hand. We shall see that suspending the lower cylinder at a depth $2q$ below the still water surface has the desired effect of rendering its motion rather small, and thus creating a relatively stable point for the upper cylinder to react against.

There are several reasonable criteria which may govern the design of a WEC. Evidently, the WEC should capture as much of the incoming wave energy as possible. At the same time, as economic viability is the prime driver behind wave energy technology, the costs should be kept low; in practical terms, this may mean that device size should be kept small. Competing with this are concerns over the survivability of the converter, which dictate that displacements of the WEC not be too large under severe conditions, favoring larger devices. We shall return to these issues in detail in later sections.

2.2. The Pierson Moskowitz spectrum

One of the most common descriptions of a sea-state for engineering purposes is the unidirectional Pierson Moskowitz (PM) spectrum, here given as a function of wavenumber k :

$$S(k) = \frac{0.00405}{k^3}\exp\left\{-0.55411\frac{g^2}{U^4k^2}\right\}, \tag{3}$$

where U is the mean wind speed at a height of 10 m above the mean surface level, and g is the gravitational acceleration. This empirically derived formula gives the energy distribution for wind waves in deep water, and differs from the JONSWAP spectrum only by the addition of a spectral–peak enhancement factor.

This spectrum (3) readily yields a number of important values associated with the sea-state:

$$H^{(1/3)} = 0.24181U^2/g, \tag{4}$$

$$k_p = 0.66570g/U^2, \tag{5}$$

where $H^{(1/3)}$ is the significant wave height and k_p is the wave number of the spectral peak for a given wind speed U. This makes it easy to present subsequent results in an alternative form when desired. A monochromatic wave with wavenumber k_p and the same wave energy density as the PM spectrum will have an amplitude

$$a_0(k_p) = 0.08549U^2/g. \tag{6}$$

For subsequent illustration it will be necessary to have some concrete, physical examples, which means specifying a sea-state via a wind speed value U. Our design conditions (denoted by a subscript d) will correspond to a wind speed $U_d = 10$ m/s, while we will consider two "severe states" (denoted by subscripts $s1$ and $s2$) with regard to the survivability, corresponding to wind speeds $U_{s1} = 15$ m/s and $U_{s2} = 20$ m/s. These are summarized in Table 1.

3. Governing equations

Our approach to solving the wave-structure problem for the twin-cylinder WEC relies on domain decomposition, which enables the use of separation of variables techniques, and eigenfunction expansion methods, whereby the solutions are developed in series of eigenfunctions (in the context of floating cylinders, see Black and Mei (1970)), who give a comprehensive description of the method, or more generally, Linton and McIver (2001), Chs.2.4.1 & 2.5.2, or Zheng et al. (2005), Secs. 2 & 3 for a recent application to floating cylinders). As the full formulation is rather lengthy, we only indicate the most important equations, and refer the interested reader to work cited above.

The fluid is assumed to be incompressible and inviscid, and the flow irrotational. Introducing a velocity potential $\Phi(r,\theta,z,t)$, and assuming periodic motion of frequency ω, the potential is separated into spatial and temporal parts,

$$\Phi(r,\theta,z,t) = \phi(r,\theta,z)e^{i\omega t}, \tag{7}$$

where $\phi(r,\theta,z)$ satisfies the Laplace equation:

$$\phi_{rr} + \frac{1}{r}\phi_r + \frac{1}{r^2}\phi_{\theta\theta} + \phi_{zz} = 0, \tag{8}$$

subject to the linearized boundary conditions on the free surface $z = 0$ and on the bed $z = -h$:

$$\phi_z - \sigma\phi = 0,\ \text{on } z = 0,\ r > R, \tag{9}$$

$$\phi_z = 0,\ \text{on } z = -h, \tag{10}$$

where $\sigma = \omega^2/g$.

At the interface between structure and fluid, the normal velocity of the structure must equal that of the adjacent fluid particles, written in terms of the potential (7):

$$\frac{\partial\Phi}{\partial n} = V_n, \tag{11}$$

where V_n is the component of the structure's velocity in the direction of the outward pointing normal vector n, which may be applied at the equilibrium surface under the assumptions of linearity. Owing to this very linearity, we continue with the well-known decomposition of the problem into two parts: one due to the waves (ϕ_S) scattered from the structure (which is assumed fixed) by the incident wave field, and one due to the waves (ϕ_R) radiated by the motion of the structure, such that $\phi = \phi_S + \phi_R$. ϕ_S is decomposed further into the potential due to the

Table 1
The wind speed U, significant wave height $H^{(1/3)}$, peak wavenumber k_p, and peak wavelength $\lambda_p = 2\pi/k_p$ associated with PM spectra used for design and survivability considerations.

	S_d	S_{s1}	S_{s2}
U (m/s)	10	15	20
$H^{(1/3)}$ (m)	2.47	5.55	9.87
k_p (1/m)	0.065	0.029	0.016
λ_p (m)	96.30	216.67	385.19

incident wave ϕ_I and that due to the waves diffracted from the fixed structure ϕ_D, where

$$\frac{\partial \phi_D}{\partial n} = -\frac{\partial \phi_I}{\partial n} \text{ on the body surface } S. \tag{12}$$

The remaining radiated part of the potential ϕ_R must then satisfy (11), where the normal velocities are to be determined from the equations of motion. We shall consider an incident monochromatic wave with amplitude a_0, so that ϕ_I is known *a priori*.

Introducing the as-yet unknown displacements of the upper ($j = 1$) and lower ($j = 2$) cylinder for the three modes of motion

$$\zeta_{zj} = \zeta_{zj0} e^{i\omega t} \text{ for heave,} \tag{13}$$

$$\zeta_{xj} = \zeta_{xj0} e^{i\omega t} \text{ for surge,} \tag{14}$$

$$\theta_j = \theta_{j0} e^{i\omega t} \text{ for pitch,} \tag{15}$$

where ζ_{zj0}, ζ_{xj0} and θ_{j0} are the complex amplitudes of the corresponding displacements, we can write the boundary condition (11) for the spatial part of the total potential ϕ in the following form:

$$\phi_z = i\omega\zeta_{z10} - i\omega\theta_{10} r\cos\theta, \quad \text{on } z = -H_1,\ r < R, \tag{16}$$

$$\phi_z = i\omega\zeta_{z20} - i\omega\theta_{20} r\cos\theta, \ \text{on } z = -(H_1+H_2),\ z = -(H_1+H_2+H_3),\ r < R \tag{17}$$

$$\phi_r = i\omega\zeta_{x10}\ \cos\theta - i\omega\theta_{10}(z_0 - z)\ \cos\theta, \quad \text{on } -H_1 < z < 0,\ r = R, \tag{18}$$

$$\phi_r = i\omega\zeta_{x20}\ \cos\theta - i\omega\theta_{20}(z_0 - z)\ \cos\theta, \quad \text{on } -(H_1+H_2+H_3) < z < -(H_1+H_2),\ r = R, \tag{19}$$

where (16) is posed on the bottom of the upper cylinder, (17) on the top and bottom of the lower cylinder, (18) on the sides of the upper cylinder, and (19) on the sides of the lower cylinder. These conditions are supplemented by Sommerfeld's radiation condition, requiring the diffracted and radiated waves to be outgoing as $r \to \infty$.

Due to the configuration of two axisymmetric floating cylinders, we must consider three fluid regions, one between the coaxial cylinders (region II), one between the lower cylinder and the bed (region III), and one outside the vertical extension of the cylinders (region I), as depicted in Fig. 2. Subsequently the scattering problem is divided into three problems, one in each subdomain, and the radiation problem for each of the three modes of each of the two cylinders is divided into three problems. The reader may appreciate the effort involved in keeping track of, solving, and subsequently matching solutions, of 21 problems for the potentials involved. These potentials are then applied in calculating the forces on the two cylinders, in the form of pressures from the surrounding fluid.

The full expressions for the exciting, hydrodynamic, and hydrostatic forces are lengthy and will not be given. We note only that we have found excellent agreement between our results and published work (Garrett, 1971; Yeung, 1981; Berggren and Johansson, 1992; Zheng et al., 2005; Bhatta, 2007, 2011; Garnaud and Mei, 2010) some of which is shown in Appendix A.

The forces due to the fluid, together with those due to the dampers are employed with Newton's second law to yield the body motions. The first two equations, (20) and (21), equate the vertical (heave) forces with the masses and accelerations of the upper and lower cylinder, respectively. The next, (22) and (23), are those for the horizontal (surge) forces. The final pair, (24) and (25), equate the torques about the $y-$axis to the angular acceleration times moment of inertia of the upper and lower cylinder, respectively.

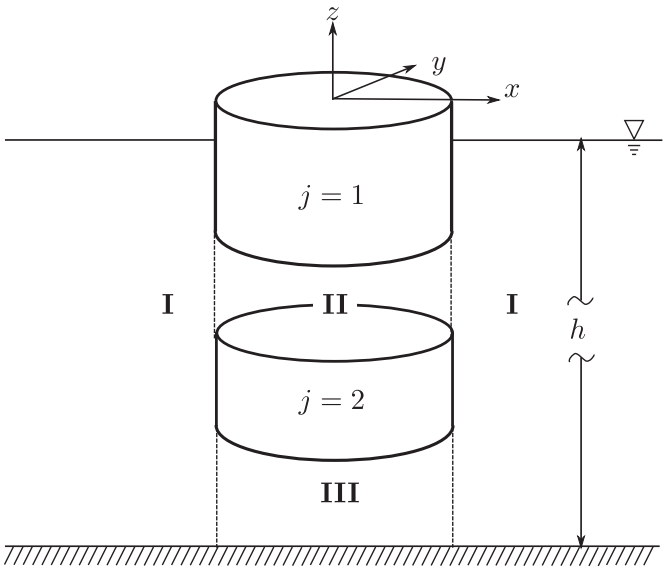

Fig. 2. Domain decomposition for the twin-cylinder problem.

$$F_{z1} + F_{z1\to z1} + F_{z2\to z1} + F_{hs,z1} + F_{d,z1} = -\omega^2\zeta_{z10}M_1, \tag{20}$$

$$F_{z2} + F_{z1\to z2} + F_{z2\to z2} + F_{hs,z2} + F_{d,z2} = -\omega^2\zeta_{z20}M_2, \tag{21}$$

$$F_{x1} + F_{x1\to x1} + F_{x2\to x1} + F_{y1\to x1} + F_{y2\to x1} = -\omega^2\zeta_{x10}M_1, \tag{22}$$

$$F_{x2} + F_{x1\to x2} + F_{x2\to x2} + F_{y1\to x2} + F_{y2\to x2} = -\omega^2\zeta_{x20}M_2, \tag{23}$$

$$F_{y1} + F_{x1\to y1} + F_{x2\to y1} + F_{y1\to y1} + F_{y2\to y1} + F_{hs,y1} + F_{d,y1} = -\omega^2\theta_{10}I_1, \tag{24}$$

$$F_{y2} + F_{x1\to y2} + F_{x2\to y2} + F_{y1\to y2} + F_{y2\to y2} + F_{hs,y2} + F_{d,y2} = -\omega^2\theta_{20}I_2, \tag{25}$$

Table 2
Notation for terms appearing in (20)–(25). Terms with subscripted x or z are forces, and terms with subscripted y are torques.

$M_i,\ i \in \{1,2\}$	Mass of cylinder i.
$I_i,\ i \in \{1,2\}$	Moment of inertia of cylinder i about the y-axis
$F_{xi},\ F_{yi},\ F_{zi},\ i \in \{1,2\}$	Exciting forces/torques on cylinder i in the x, y, and z directions
$F_{\alpha i\to\beta j}, i,j \in \{1,2\},\ \alpha,\beta \in \{x,y,z\}$	Hydrodynamic force/torque of the α motion of cylinder i in the β direction of cylinder j.
$F_{hs,yi},\ F_{hs,zi},\ i \in \{1,2\}$	Hydrostatic forces/torques in the y and z direction on cylinder i.
$F_{d,yi},\ F_{d,zi},\ i \in \{1,2\}$	Forces/torques caused by the damping system in the y and z direction on cylinder i.
$\zeta_{xi0},\ \zeta_{zi0},\ \theta_{i0},\ i \in \{1,2\}$	Displacement amplitudes of cylinder i in surge (ζ_x), heave (ζ_z), and pitch (θ).

The terms appearing in the above equations are given in Table 2.

The masses and moments of inertia have the explicit form (see (1) and (2))

$$M_1 = M_2 = \rho\pi q^3,$$

$$I_1 = \frac{73}{108}\rho\pi q^5,$$

$$I_2 = \frac{757}{108}\rho\pi q^5,$$

and the damping forces are

$$F_{d,z1} = -i\omega C(\zeta_{z10} - \zeta_{z20})e^{i\omega t},$$

$$F_{d,z2} = i\omega C(\zeta_{z10} - \zeta_{z20})e^{i\omega t},$$

$$F_{d,y1} = -\frac{1}{2}i\omega CR^2(\theta_{10} - \theta_{20})e^{i\omega t},$$

$$F_{d,y2} = \frac{1}{2}i\omega CR^2(\theta_{10} - \theta_{20})e^{i\omega t}.$$

After the displacements of the cylinders are obtained, the captured power can then be calculated as follows:

$$P_a = \frac{1}{2}C\omega^2(\zeta_{z10} - \zeta_{z20})(\zeta^*_{z10} - \zeta^*_{z20}) + \frac{1}{4}C\omega^2R^2(\theta_{10} - \theta_{20})(\theta^*_{10} - \theta^*_{20}), \tag{26}$$

where ζ^*_{zj0} and θ^*_{j0} are the complex conjugates of ζ_{zj0} and θ_{j0}, respectively.

4. Design of the WEC for monochromatic waves

We now undertake to examine the design of the WEC, based on the three parameters characterizing the environmental conditions ρ, g, and U, the two WEC parameters q and C, and the seven WEC performance parameters calculated from the wave-structure interaction problem P_a, ζ_{x10}, ζ_{x20}, ζ_{z10}, ζ_{z20}, θ_{10} and θ_{20}. An application of Buckingham's π theorem (Crowe et al., 2001) yields nine dimensionless quantities that characterize this problem: $\frac{q}{U^2/g}$, $\frac{C}{\rho U^5/g^2}$, $\frac{P_a}{\rho U^7/g^2}$, $\frac{\zeta_{zj0}}{U^2/g}$, $\frac{\zeta_{xj0}}{U^2/g}$, and θ_{j0}, where $j \in \{1,2\}$ again denotes the upper and lower cylinder, respectively. In the sequel, we will make use of a $\sim$ to denote nondimensional variables, i.e., the nine dimensionless quantities above will be $\tilde{q}$, $\tilde{C}$, $\tilde{P_a}$, $\tilde{\zeta}_{zj0}$, $\tilde{\zeta}_{xj0}$, and $\tilde{\theta}_{j0}$.

4.1. The WEC in heave motion under a monochromatic wave

For simplicity of presentation and ease of understanding we initially consider only the heave mode, motivated by the fact that, while surge and pitch are coupled, they are both independent of heave. The response of the WEC under incoming monochromatic waves is first considered, where our physical test-case corresponds to a monochromatic wave of wavelength 96.3 m (equal to that at the peak of the design spectrum S_d) and an amplitude $a_d = 0.87$ m, such that the total energy density of the wave is equal to that of S_d, see (6) and Table 1.

4.1.1. Step 1: determination of the WEC's size

We first choose the dashpot coefficient C to be zero, which means that the two cylinders are freely floating. In this case, once the incident monochromatic wave is given, the only WEC parameter to be determined is q. Dimensional analysis can then be applied to the problem of determining the quantity of interest q for the motions of the upper cylinder ζ_{z10} and the lower cylinder ζ_{z20} separately. Once again, Buckingham's π theorem yields that, for the variables ρ, g, U, q, and ζ_{zj0}, there exist exactly two nondimensional quantities, which must be related by a relation

$$\tilde{\zeta}_{zj0} = \Psi_{1j}(\tilde{q}). \tag{27}$$

The maximum displacement of the cylinder j as a function of size $\tilde{q}$ thus corresponds to the extrema of Ψ_1. Equation (27) is plotted in Fig. 3 for the upper and lower cylinders.

As we are ultimately interested in relative displacements of the cylinders, the global maximum of Ψ_{11} ($\tilde{\zeta}_{z10}$) and the local maximum of Ψ_{12} ($\tilde{\zeta}_{z20}$) which occur at $\tilde{q} = 0.97$ yield the chosen design size.

4.1.2. Step 2: determination of the dashpot coefficient C

The maximum displacement in Fig. 3 is related to the resonance between the cylinders and the incident monochromatic wave. The introduction of a damper, while changing the magnitude of the displacement, can be shown to have no effect on the location of the resonant maximum, which remains $\tilde{q} = 0.97$ (see Fig. 3) even for various values of C. Thus, the size of the WEC determined from the freely floating case is used to specify the damping coefficient C.

Given the unique relationship between q and ζ_{zj0}, independent of C, described above, the dimensional analysis yields an equation

$$\tilde{P}_a = \Psi_2(\tilde{C}; \tilde{q}), \tag{28}$$

where Ψ_2 is plotted in Fig. 4 for the WEC size as determined in the last section ($\tilde{q} = 0.97$).

We elect to determine the dashpot coefficient C from the maximum of captured power P_a in Fig. 4, calculated from the heave terms only in (26). This results in $\tilde{C} = 0.32$ and $\tilde{P}_a = 0.0034$.

Thus, the WEC design for a monochromatic wave has been determined. Taking the design wave introduced in the beginning of Section 4 as a physical example, the WEC has the dimensions $q = 9.9m$ and $C = 3.3 \times 10^5 Ns/m$, and can capture $P_a = 3.5 \times 10^5$ Watt from a monochromatic wave 96.3 m long and 0.87 m in amplitude.

4.2. General motions of the WEC in monochromatic waves

Having treated the simpler case of heave-only motion, we now consider the general case in which the WEC is additionally allowed to undergo surge and pitch motions. Akin to the previous section which only dealt with the heave motion, the design procedure of the WEC in the general case is also divided into two steps, as illustrated in detail below.

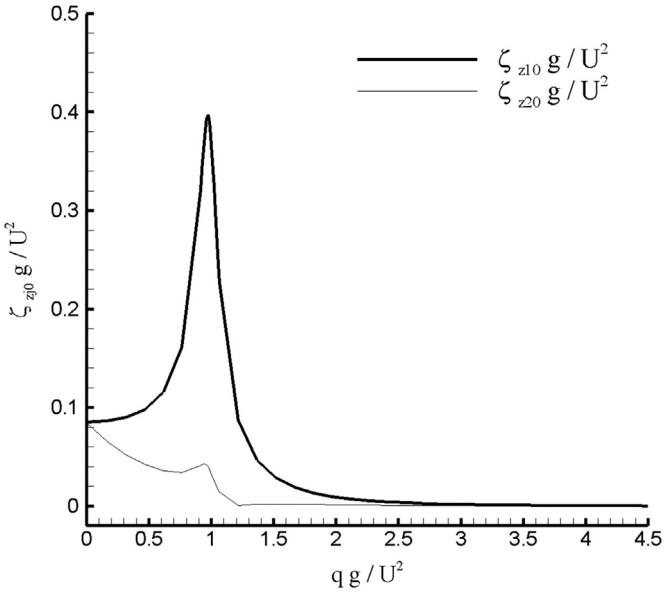

Fig. 3. Displacement amplitudes for each of the two freely floating cylinders ($C = 0$) under the design monochromatic wave. $\tilde{\zeta}_{z10}$: upper cylinder, thick line; $\tilde{\zeta}_{z20}$: lower cylinder, thin line.

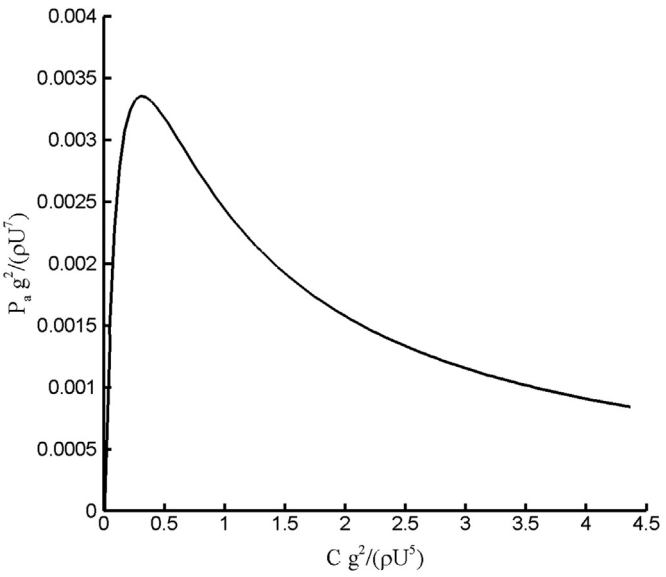

Fig. 4. The relationship between the captured power $\tilde{P}_a$ and the dashpot coefficient $\tilde{C}$ for the heave motion induced by the design monochromatic wave, where $\tilde{q} = 0.97$.

4.2.1. Step 1: determination of the WEC's size q

We start once again with the freely floating case, where the dashpot coefficient $C = 0$. Using the equations of motion (20)–(25), we can obtain the displacements of the two cylinders in the x and z directions, and the angle around the y axis.

Once the monochromatic wave is given, or equivalently, once the mean wind speed for the corresponding PM spectrum is given (recall that this can be used to specify a monochromatic wave for design purposes by (6)), the physical process of determining the size of the WEC can be written in the following dimensionless form:

$$\tilde{\zeta}_{zj0} = \Psi_{1j}(\tilde{q}), \tag{29}$$

$$\tilde{\zeta}_{xj0} = \Psi_{2j}(\tilde{q}), \tag{30}$$

$$\theta_{j0} = \Psi_{3j}(\tilde{q}), \tag{31}$$

where ζ_{zj0} and ζ_{xj0} denote the amplitudes of the vertical and horizontal displacements respectively, θ_{j0} is the amplitude of the angle around the y axis, and $j = 1, 2$ corresponds to the upper and lower cylinder, respectively. We now seek the maxima of the functions Ψ_{1j}, Ψ_{2j} and Ψ_{3j}, which correspond to the six curves presented in Fig. 5.

Due to the increase in number of modes, the picture of the displacements is more complex than in the preceding section. It may be observed that the heave mode is decoupled from the surge and pitch modes, yielding again the global maximum at $\tilde{q} = 0.97$. The surge and pitch modes are coupled, and are observed to present a global maximum for relative displacement at $\tilde{q} = 0.61$, resulting in an ambiguous situation for determining the size of the WEC.

4.2.2. Step 2: determination of the dashpot coefficient C

As in the preceding section, we now suppose that the size of the WEC is given. The captured power P_a then depends on the dashpot coefficient C. The determination of optimal power absorption as a function of dashpot coefficient is described in dimensionless form by

$$\tilde{P}_a = \Psi_4(\tilde{C}; \tilde{q}), \tag{32}$$

where, as we have seen, there is some flexibility in choice of q. The function Ψ_4 is plotted in Fig. 6 for both $\tilde{q} = 0.61$ and $\tilde{q} = 0.97$. For the device operating optimally in heave ($\tilde{q} = 0.97$, thick line) there is a unique maximum at $\tilde{C} = 0.34$ with $\tilde{P}_a = 0.0035$ (denoted Case E), very close to the heave-only case discussed in Section 4.1. For the pitch–surge optimized device ($\tilde{q} = 0.61$, thin line) there are two local maxima $\tilde{C} = 0.035$ and $\tilde{C} = 1.34$, with corresponding $\tilde{P}_a = 0.0012$ and 0.0013, (denoted Case A1 and A2, respectively).

The situation for monochromatic incident waves is summed up in Table 3 which shows the nondimensional size, optimal damping, captured power, and displacement amplitudes for the cases discussed above. As we have observed, introducing pitch and surge motions leads to a two-fold branching in the design procedure. Firstly, in free motion, one value of $\tilde{q}$ is found to yield the largest pitch and surge displacements, while another value yields the largest heave displacements. While the heave-optimized case has a unique maximum $\tilde{P}_a$ as a function of damping, the pitch/surge-optimized case admits two local maxima of $\tilde{P}_a$, one with relatively low, the other with relatively high damping $\tilde{C}$, compared to the heave case (see Fig. 6).

This opens up the possibility that the overall optimal design may not coincide with a design optimized for pitch/surge or heave alone, but

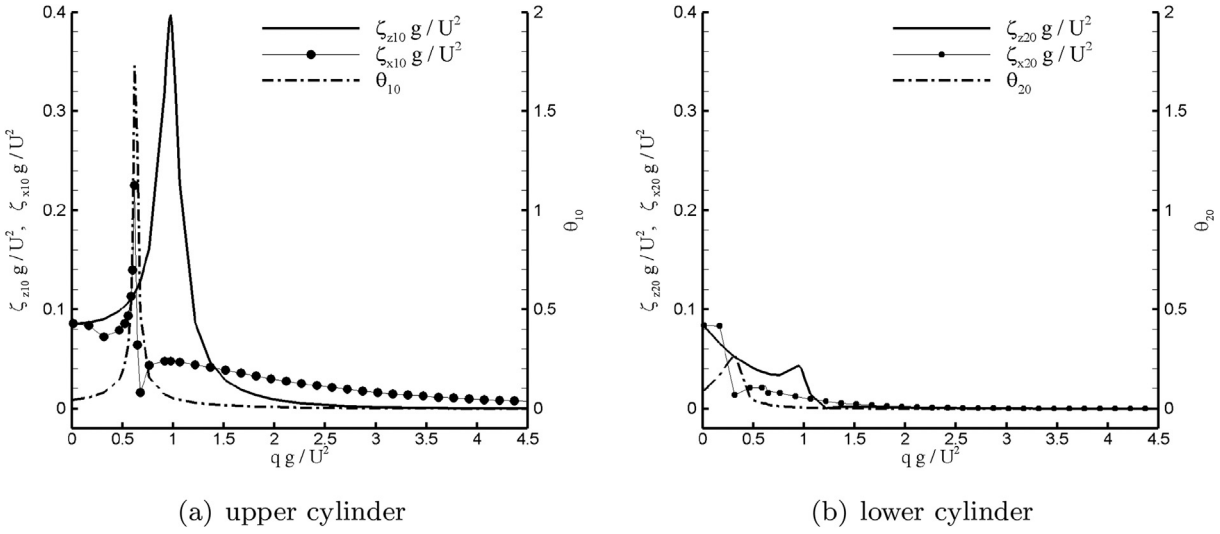

(a) upper cylinder (b) lower cylinder

Fig. 5. Displacement amplitudes of the two freely-floating cylinders ($C = 0$) in heave, surge and pitch under the design monochromatic wave. $\tilde{\zeta}_{zj0}$: amplitude of the vertical displacement; $\tilde{\zeta}_{xj0}$: amplitude of the horizontal displacement; θ_{j0}: amplitude of the angle around the y axis. $j = 1, 2$ correspond to the upper and lower cylinders, respectively.

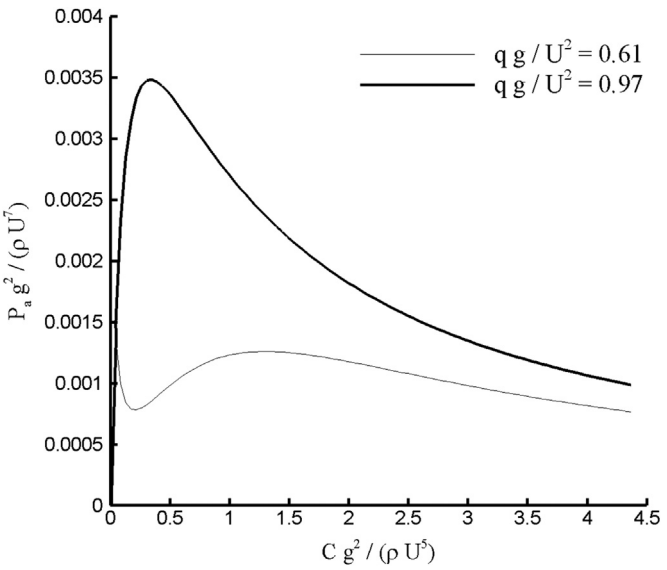

Fig. 6. The captured power P_a of the WEC in the combined motions versus the damping coefficient C. Thin line: $\frac{q}{U^2/g} = 0.61$; thick line: $\frac{q}{U^2/g} = 0.97$.

occupying some middle ground. The performance of such intermediate devices (Cases B, C, and D), as well as devices somewhat larger than Case E (Cases F, G and H) is explored for the monochromatic design wave in Table 3. In each of Cases B through H, a damping C has been chosen to maximize the captured power.

Here we see that a shift in device size from the smaller, primarily pitching/surging devices, towards larger, primarily heaving devices has a positive impact on captured power, up to device E. Thereafter, an increase in device size leads to a reduction in captured power, as the larger devices operate preferentially at smaller wavenumbers.

This situation is depicted in Fig. 7, which shows $\tilde{P}_a^* \equiv P_a^*/(\rho U^3)$, the dimensionless captured power per unit wave amplitude squared, where $P_a^* \equiv P_a/a_0^2$. To illustrate the associated displacements, Fig. 8 shows the displacement in heave for the upper cylinder ζ_{z10} divided by a_0. Note that for case A1, the maximum value of $\zeta_{z10}(k)/a(k)$ is 4.4 (not shown).

5. Design of the WEC for a PM spectrum

Up to this point, we have considered WEC design for monochromatic waves. In brief: a given wind speed U determines the two necessary parameters, wavenumber k_p and amplitude a_0 from (6). With a monochromatic wave fully described by (k_p, a_0), we may initially assume freely floating cylinders, and choose their size $\tilde{q}$ for maximum displacement in pitch and surge (as these modes are coupled), for maximum displacement in heave, or at some intermediate value. In each case, a damping $\tilde{C}$ is chosen to maximize the captured power for this incident design wave, leading to the cases A1 through H above. As demonstrated in Figs. 7 and 8, the motions and performance of a device designed for a wave $(k_p, a_0(k_p))$ may change considerably for other waves.

For practical reasons, our primary interest must be focused on irregular waves, where we may elect to tune the device to operate optimally at the peak of the spectrum, but must consider its performance for a broad band of incident waves. Under irregular waves it is no longer possible to give a single value for the displacements of each floating cylinder. We begin with some preliminaries regarding the behavior of the WEC in irregular seas.

For a monochromatic wave, the absorbed power P_a (see (26)) and displacements $\zeta_{\alpha j0}$ and θ_{j0} are given by

$$P_a(q, C, k, a_0) \equiv a_0^2 P_a^*(q, C, k),$$

$$\zeta_{\alpha j0}(q, C, k, a_0) \equiv a_0 \widehat{A}_{\alpha j}(q, C, k),$$

$$\theta_{j0}(q, C, k, a_0) \equiv a_0 \widehat{A}_{yj}(q, C, k).$$

where $j = 1, 2$ denotes the upper and lower cylinders, P_a^* is the absorbed power per unit wave amplitude square, and $\widehat{A}_{\alpha j}$ with $\alpha \in \{x, y, z\}$ denote the relative amplitudes of surge, pitch and heave motions, respectively. For a given spectrum $S(k)$ the total absorbed power by a device of type (q, C) is

$$P_a^{\text{total}} = \int_0^\infty 2P_a^*(k)S(k)dk. \tag{33}$$

Just as the spectrum describes the distribution of wave energy among different frequencies, and allows for statistical inferences such as a definition of the significant wave-height, so analogously we may consider a *displacement spectrum*

$$E_{\alpha j}(k) \equiv S(k)\left(\widehat{A}_{\alpha j}\right)^2, \tag{34}$$

and define the *significant displacement* by

$$H_{\alpha j}^{1/3} = 4 \cdot \left(\int_0^\infty E_{\alpha j}(k)dk\right)^{1/2}. \tag{35}$$

Here $H_\alpha^{(1/3)}$ $(\alpha = x, y, z)$ is the distance from the displacement's trough to crest and

$$\zeta_{zj0}^{(1/3)} = \frac{1}{2}H_{zj}^{(1/3)}, \tag{36}$$

$$\zeta_{xj0}^{(1/3)} = \frac{1}{2}H_{xj}^{(1/3)}, \tag{37}$$

$$\theta_{j0}^{(1/3)} = \frac{1}{2}H_{yj}^{(1/3)}, \tag{38}$$

are the so-called "significant amplitudes of the displacement" in z and x directions, and the angle around the y axis, respectively.

Applying the concepts developed above to the problem of power absorption from an incident, broad-banded sea, we evaluate the above expressions for the spectra introduced in Section 2. The results are given

Table 3
The size, damping, captured power and displacement of 3-mode WECs in monochromatic waves.

Cases:	A1	A2	B	C	D	E	F	G	H
$\tilde{q}$	0.61	0.61	0.70	0.79	0.88	0.97	1.06	1.15	1.24
$\tilde{C}$	0.035	1.34	0.90	0.67	0.51	0.34	0.56	1.09	1.91
$\tilde{P}_a$	0.0012	0.0013	0.0015	0.0021	0.0028	0.0035	0.0028	0.0020	0.0015
$\tilde{\zeta}_{z10}$	0.11	0.089	0.093	0.11	0.14	0.19	0.13	0.063	0.039
$\tilde{\zeta}_{z20}$	0.036	0.053	0.033	0.026	0.023	0.021	0.0097	0.0042	0.0031
$\tilde{\zeta}_{x10}$	0.12	0.063	0.060	0.055	0.050	0.048	0.047	0.040	0.038
$\tilde{\zeta}_{x20}$	0.018	0.016	0.015	0.013	0.012	0.011	0.0093	0.0069	0.0057
$\theta_{10}(rad)$	0.70	0.041	0.052	0.069	0.068	0.056	0.042	0.028	0.022
$\theta_{20}(rad)$	0.028	0.031	0.021	0.014	0.0094	0.0066	0.0051	0.0035	0.0027

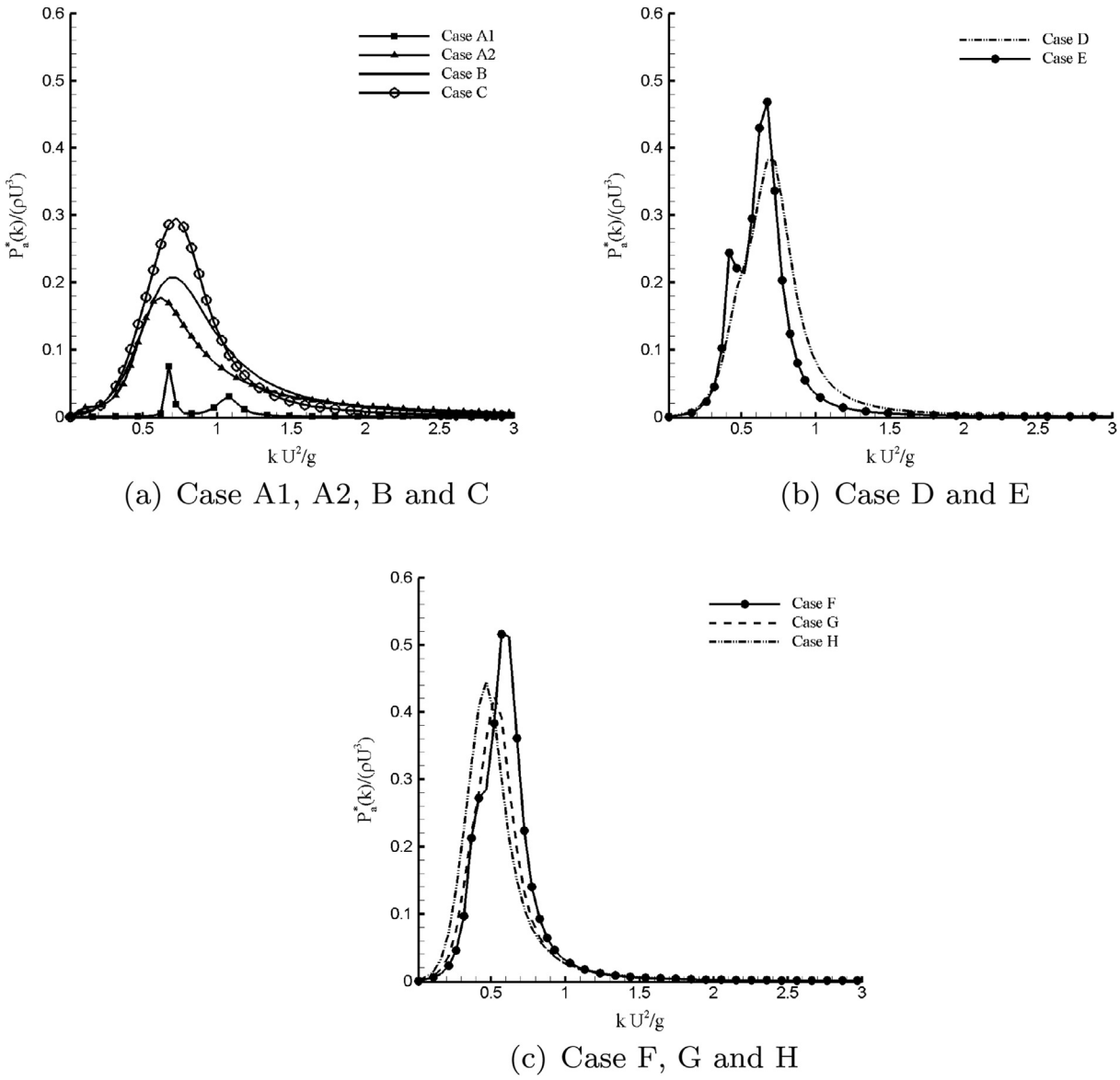

Fig. 7. The dimensionless captured power per unit wave amplitude square $P_a^*(k)/(\rho U^3)$ under different monochromatic waves as a function of wavenumber.

in nondimensional form in Table 4, which shows the captured power and displacement amplitudes for the spectra S_d, S_{s1} and S_{s2}, nondimensionalized by $U = U_d$. This may be compared to the analogous Table 3 for the monochromatic case. In the following section, we turn to a discussion of these results.

6. Discussion

Numerous competing criteria exist in determining WEC size, of which we shall consider only power capture, which naturally should be maximized, and survivability as assessed from the device motions. Note that the Cases A1 through H above are ordered by increasing size q which may be assumed correlated to the cost per *device,* all other things being equal. Due to the burgeoning state of wave energy technology, it seems premature to speculate any further about cost, given that it depends not only on device size, but also design specifics such as materials and component costs, as well as costs related to regular maintenance or major overhaul, both factors which will in turn be affected by size.

6.1. Power capture

The most straightforward metric to evaluate is the power captured by a WEC. For a design PM spectrum S_d corresponding to a wind speed $U_d =$ 10 m/s, and severe spectra S_{s1} and S_{s2} corresponding to $U_{s1} = 15$ m/s (energy density of 18.7 kJ/m^2) and $U_{s2} = 20$ m/s (energy density of 59.6 kJ/m^2), respectively, the dimensional size, damping and absorbed power of WECs A1 through H are presented in Table 5.

The picture which emerges from comparing the absorbed powers in the monochromatic and spectral cases is quite striking. While the narrow-banded response of device A1 (see Fig. 8(a)) yields a performance comparable to slightly larger devices for monochromatic waves, power absorption is dramatically lower for an incident PM spectrum. Likewise, though the heave-optimized device E is clearly superior to devices of similar size (D and F) for monochromatic waves, this situation sees a dramatic reversal in the case of incident irregular waves. That devices either larger or smaller than the heave-optimum outperform it for irregular seas clearly demonstrates the pitfalls of a design based on monochromatic waves.

Dimensional values of captured power are also provided for the two severe spectra, S_{s1} and S_{s2}. As expected, the larger devices benefit most

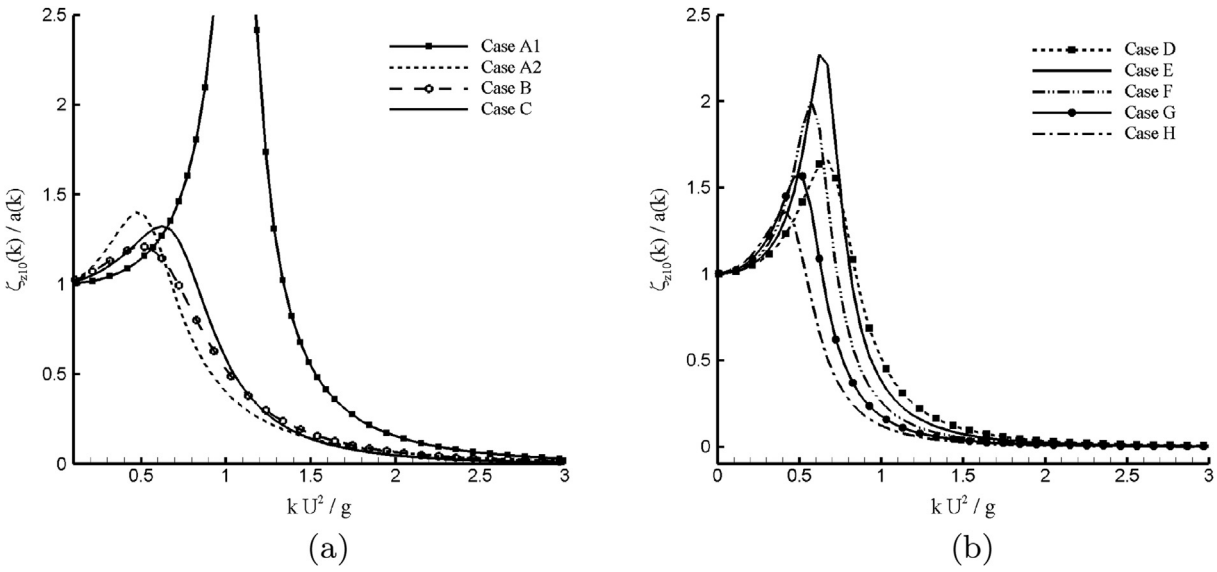

Fig. 8. The dimensionless displacement $\widehat{A}_{z1} = \zeta_{z10}/a_0$ of the upper cylinder in the combined motions under different monochromatic waves.(a)vertical displacement of cases A1, A2, B and C; (b)vertical displacement of cases D, E, F, G and H.

Table 4
The dimensionless captured power $\bar{P}_a^{\text{total}}$ along with nondimensional significant amplitudes of displacement in heave $\bar{\zeta}_{zj0}^{(1/3)}$, surge $\bar{\zeta}_{xj0}^{(1/3)}$, and pitch $\theta_{j0}^{(1/3)}$ (rad), for the WECs A1 through H attacked by a design spectrum S_d, a severe spectrum S_{s1} ($U_{s1} = 1.5U_d$), and a second severe spectrum S_{s2} ($U_{s2} = 2U_d$).

Cases:	A1	A2	B	C	D	E	F	G	H
$\bar{q}$	0.61	0.61	0.70	0.79	0.88	0.97	1.06	1.15	1.24
$\bar{C}$	0.035	1.34	0.90	0.67	0.51	0.34	0.56	1.09	1.91
S_d									
$\bar{P}_a^{\text{total}}$	7.01×10^{-5}	0.00065	0.00081	0.0010	0.0011	0.0010	0.0011	0.00089	0.00086
$\bar{\zeta}_{z10}^{(1/3)}$	0.22	0.097	0.096	0.11	0.12	0.14	0.12	0.094	0.071
$\bar{\zeta}_{z20}^{(1/3)}$	0.044	0.065	0.040	0.030	0.027	0.025	0.021	0.017	0.013
$\bar{\zeta}_{x10}^{(1/3)}$	0.10	0.077	0.073	0.068	0.064	0.059	0.056	0.054	0.051
$\bar{\zeta}_{x20}^{(1/3)}$	0.022	0.019	0.018	0.016	0.015	0.014	0.012	0.011	0.0093
$\theta_{10}^{(1/3)}$	0.60	0.050	0.059	0.073	0.084	0.096	0.068	0.045	0.032
$\theta_{20}^{(1/3)}$	0.012	0.015	0.0093	0.0058	0.0039	0.0027	0.0020	0.0016	0.0012
S_{s1}									
$\bar{P}_a^{\text{total}}$	0.00016	0.0025	0.0030	0.0037	0.0043	0.0046	0.0061	0.0060	0.0074
$\bar{\zeta}_{z10}^{(1/3)}$	0.37	0.31	0.29	0.29	0.32	0.35	0.34	0.31	0.29
$\bar{\zeta}_{z20}^{(1/3)}$	0.15	0.25	0.18	0.14	0.13	0.12	0.11	0.11	0.10
$\bar{\zeta}_{x10}^{(1/3)}$	0.25	0.21	0.22	0.21	0.21	0.21	0.20	0.19	0.19
$\bar{\zeta}_{x20}^{(1/3)}$	0.090	0.076	0.081	0.081	0.078	0.075	0.070	0.065	0.060
$\theta_{10}^{(1/3)}$	0.98	0.16	0.14	0.17	0.21	0.29	0.23	0.16	0.12
$\theta_{20}^{(1/3)}$	0.13	0.17	0.11	0.075	0.058	0.046	0.039	0.034	0.029
S_{s2}									
$\bar{P}_a^{\text{total}}$	0.00019	0.0044	0.0049	0.0056	0.0064	0.0068	0.0097	0.011	0.014
$\bar{\zeta}_{z10}^{(1/3)}$	0.55	0.54	0.51	0.52	0.53	0.56	0.56	0.54	0.53
$\bar{\zeta}_{z20}^{(1/3)}$	0.34	0.47	0.39	0.33	0.30	0.29	0.28	0.27	0.27
$\bar{\zeta}_{x10}^{(1/3)}$	0.45	0.42	0.42	0.42	0.42	0.42	0.42	0.41	0.40
$\bar{\zeta}_{x20}^{(1/3)}$	0.20	0.19	0.19	0.20	0.20	0.19	0.19	0.18	0.17
$\theta_{10}^{(1/3)}$	1.07	0.317	0.21	0.22	0.27	0.37	0.31	0.24	0.19
$\theta_{20}^{(1/3)}$	0.31	0.40	0.25	0.18	0.14	0.12	0.10	0.088	0.077

from this increased wave resource, while a sea composed of increasingly long waves (λ_p for S_{s1} is 217 m, and for S_{s2} is 385 m, see Table 1) begins to saturate the power capture capabilities of the smallest devices. In the following sections on survivability and grading of WECs, we shall explore the feasibility of operating WECs in such large sea states.

6.2. Survivability

Assessing WEC survivability is less clear-cut than assessing power capture. It is clear that WECs must be robust in design, as during a ten-year operational period a converter may expect to encounter some tens of millions of waves. During particularly severe sea-states, power production will need to be halted in order to avoid damage to the device or

Table 5
Dimensional absorbed power P_a (Watt) for cases A1 through H, for an incoming monochromatic wave (P_a^m) and the design PM spectrum with $U = 10$ m/s (P_a^d), both with the same energy density of 3.7 KJ/m^2. Also given are the absorbed power for the severe spectra S_{s1} (P_a^{s1}) and S_{s2} (P_a^{s2}).

Cases:	A1	A2	B	C	D	E	F	G	H
q [m]	6.2	6.2	7.1	8.1	9.0	9.9	10.8	11.4	12.7
C ($\cdot 10^5$) [Ns/m]	0.364	14.0	9.37	6.98	5.31	3.54	5.83	11.3	19.9
$P_a^m(\cdot 10^5)$ [W]	1.25	1.35	1.56	2.19	2.92	3.64	2.92	2.08	1.56
$P_a^d(\cdot 10^5)$ [W]	0.0730	0.672	0.849	1.04	1.14	1.06	1.17	0.931	0.893
$P_a^{s1}(\cdot 10^5)$ [W]	0.165	2.65	3.13	3.80	4.43	4.77	6.36	6.27	7.73
$P_a^{s2}(\cdot 10^5)$ [W]	0.197	4.62	5.09	5.88	6.67	7.10	10.1	11.0	15.0

Table 6
Relative heave displacements versus draft $\zeta_z^r = (\zeta_{z10}^{(1/3)} - \zeta_{z20}^{(1/3)})/q$, and relative pitch displacement $\theta^r = \theta_{10}^{(1/3)}/(\pi/2)$.

	A1	A2	B	C	D	E	F	G	H
S_d									
ζ_z^r	0.29	0.05	0.08	0.10	0.11	0.12	0.09	0.07	0.05
θ_1	0.38	0.03	0.04	0.05	0.05	0.06	0.04	0.03	0.02
S_{s1}									
ζ_z^r	0.36	0.10	0.16	0.19	0.22	0.24	0.22	0.18	0.15
θ_1	0.62	0.10	0.09	0.11	0.13	0.18	0.15	0.10	0.08
S_{s2}									
ζ_z^r	0.34	0.11	0.17	0.24	0.26	0.28	0.26	0.24	0.21
θ_1	0.68	0.20	0.13	0.14	0.17	0.24	0.20	0.15	0.12

Entries marked red exceed the maximum allowed relative vertical travel of q/3, or the maximum allowable pitch of 30°. Vertical travel between q/4 and q/3, or a pitch between 22.5° and 30° is marked orange, while a vertical travel between 0.15q and 0.25q, or a pitch between 13.5° and 22.5° is marked yellow. Smaller device motions in both pitch and heave are marked green.

loss of station-keeping.

Other authors (e.g. Maisondieu (2015) or Brown et al. (2010)) have imposed strict, ad-hoc cut-offs in $H^{(1/3)}$ for a WEC to enter "survival mode". In contrast, we propose an example framework for survivability for the twin-cylinder WEC in the three spectral sea states considered, which is presented in Table 6. The maximum allowed relative vertical travel $\zeta_{z10}^{(1/3)} - \zeta_{z20}^{(1/3)}$ is limited to $q/3$, while the maximum allowable pitch is 30°. Those cases which exceed these values are marked red (PDF only). A vertical travel between $q/4$ and $q/3$ or a pitch between 22.5° and 30° is marked orange, while a vertical travel of between $0.15q$ and $0.25q$ or a pitch between 13.5° and 22.5° is marked yellow (PDF only). Device motions smaller than these are marked green (PDF only). Recall that these nondimensional quantities depend only on the relations $U_{s1} = 1.5 \cdot U_d$ and $U_{s2} = 2 \cdot U_d$ as specified in Section 2, and the concomitant changes in significant wave-height and peak wavenumber.

For illustrative purposes, if the design spectrum S_d is generated by a fresh breeze ($U_d = 10m/s$, or 5 Beaufort, 2.47 m $H^{(1/3)}$), then the first severe state S_{s1} may be thought generated by a high wind (7 Beaufort, 5.5 m $H^{(1/3)}$). The second severe state S_{s2} occurs under conditions between gale and severe gale (8–9 Beaufort, 9.9 m $H^{(1/3)}$). These extremely harsh conditions represent an energy density more than 16 times that of the design spectrum, and may be expected to challenge the device design. Note that the nondimensional form of the results allows for a free choice of U_d depending on the conditions of interest.

While the increase in significant wave-height between the design spectrum S_d and the severe case S_{s2} may seem dramatic, there is no doubt that such conditions will be encountered within the operational life of a WEC. For example, while deep water conditions for the Eastern Mediterranean off Israel's coasts may see significant wave heights greater than 2 m only 6% of the time, and wave heights in summer rarely exceed 1–1.5 m, nevertheless storms with $H^{(1/3)}$ in excess of 5 m occur almost yearly. The 10-year return period significant wave height is nearly 7 m, which clearly falls within the expected operational life of a converter.

From a pure survivability standpoint, it is immediate only that the smallest converter A1 is not viable. In particular, the very small damping of this configuration (see Table 5), while allowing for efficient power capture from the pitch mode, also leads to overly large displacements even for design conditions. With survivability as the central aim of design, larger structures will necessarily fare better, though the differences between devices D, E, and F are in practice rather small.

Ultimately, WEC survivability must be examined not just via linear theory, but also take into account such highly nonlinear factors as wave impacts on structures (see e.g. Akrish et al. (2016)). In addition, there is some chance that survivability may be underestimated due to the neglect of viscous terms in the equations of motion (see Cummins and Dias, 2017). Nevertheless, the present estimates of the significant displacements give some initial indication of when a device should be forced to cease normal power production.

6.3. Grading WEC sizes

We now make a preliminary attempt to sum up the results of the preceding sections. The intricacies of WEC economics, as well as the many factors which are outside the scope of the present study, such as moorings, specifics of the PTO, control strategies, power conversion and transmission, and other environmental factors from seasonal variability to extreme events, will need to be taken into account for a fuller analysis. For specific full-fledged designs, detailed information about performance and survival may be sought through tank testing of scaled devices and CFD simulations (see e.g. (Göteman et al., 2015)). In addition, WEC cost will be considered, and is likely to impact significantly the ultimate design.

The lessons to be drawn from our comparison will likely change as wave-power technology matures. In a parallel with the development of wind power over the past four decades, current commercial and prototype oscillating-body WECs may be rather small, and situated in shallow water with the intention of keeping costs down. It may be expected that future developments will lead naturally to a move into the more powerful wave-regimes further offshore (see Stiassnie et al. (2016) for a discussion).

As an example, while there is a 15% reduction in absorbed power between Case E and Case H (coincident with a 24% increase in radius q) under the design spectrum, the corresponding increase in absorbed power for severe case S_{s2} is upwards of 60%. The fact that, off the Eastern Mediterranean Coast, some 45% of average wave power comes during storm events that occur only 5% of the time indicates the utility of the larger design (Kroszynski and Stiassnie, 1979). This is compounded by the increase in potential survivability of the larger devices as indicated in the previous section. On the other hand, focusing on less frequent,

high-energy sea-states may mean that the WEC is operating below capacity for significant portions of time.

Depending on the variability of the wave-energy resource, more or less weight may ultimately be given to each of the considerations just outlined. The fact that the larger devices exhibit smaller relative motions may also be a benefit for their reliability, in terms of limiting loading during normal operation. Ultimately, an effort will have to be made to weigh the additional cost of a larger device against the increase in survivability. Both of these in turn will need to be weighed against the potential of continuing operation during high-energy events, while sustaining a slight performance decrease for low-energy sea states.

7. Conclusions

We have investigated in detail the hydrodynamics of a model WEC consisting of two floating, axisymmetric cylinders connected at their upper and lower perimeters by a continuously distributed damper – allowing power capture from heave and pitch modes. The present work addresses for the first time a twin cylinder WEC allowed to move in three degrees of freedom. The inclusion of a floating, submerged cylinder as a mechanical reference for power extraction makes this design viable in the deep water, which may be expected to become even more relevant with the move to more energy-rich offshore environments (Stiassnie et al., 2016).

Our design procedure initially focused on optimizing device behavior in monochromatic waves. In the heave-only case, a device with size parameter q and damping parameter C tuned to the resonant maximum of a freely floating body outperformed all others. Allowing the device also to surge and pitch was seen to introduce additional complexity, and a differentiation was observed between devices operating preferentially in pitch/surge and those operating preferentially in heave.

Despite the multiplicity of possible designs when the device is allowed to undergo heave, surge, and pitch motions, the monochromatic case presents a clear picture from the standpoint of power absorption: the device closest to heave resonance is found to perform best. This conclusion is an artifact of the idealization represented by the monochromatic theory – a fact established by the subsequent investigation of WEC performance under an irregular sea.

For our design purposes, a Pierson-Moskowitz spectrum, characterized by wind speed, was chosen to evaluate the designs obtained from the monochromatic case. Under this spectrum, the maxima of absorbed power were found to shift markedly with respect to the monochromatic case, reflecting the need for separate design considerations for real sea states. Larger values of absorbed power under the design spectrum were found for devices both slightly larger and slightly smaller than the monochromatic optimum, raising the question of how to determine device sizing in light of other criteria.

To this end, we have devised some example metrics for grading the sizes of our twin-cylinder WEC. We have presented an example approach to quantitatively evaluate the competing aims of survivability and power extraction within the framework of our floating twin-cylinder device. This relies on a novel estimation of WEC displacements under irregular seas, which we have termed “significant displacement,” and goes beyond simply ceasing production for a certain significant wave-height. Here such considerations are presented for the single WEC case, but as the technology matures and large arrays of WECs become more practical, their layouts will also be subjected to optimization for power capture (see (McGuinness and Thomas, 2015, 2016; Fitzgerald and Thomas, 2007)) and potentially WEC survival as well.

To a certain extent all renewable energy technologies, WECs among them, cannot control their operating conditions, but must work within their environment, subject to the resulting fluctuations of the resource. It must be expected that, like wind turbines, oscillating body WECs will be designed with a “survival mode”, when normal operation cease, and the device changes its characteristics in order to avoid extreme loads. (Overtopping WECs or oscillating water-columns, due to a different working principle and resulting size, will likely have a very different survivability analysis than oscillating body designs.) This may mean increasing the damping, altering the water plane area or mass (see Stallard et al. (2009)), or other approaches (see Coe and Neary (2014)). Due to the nascent state of commercial wave-energy technology, it is difficult to offer concrete design recommendations based on the results for floating twin-cylinders. Our discussion does bear out the fact that a slight over-engineering may be preferable, given the large relative contribution of infrequent, high-energy events to the annual energy budget at many sites, and the demands of survival and robustness. We believe these results to be applicable more broadly to oscillating-body converters, constrained in size as they are by the incident wavelength, indicated by the striking similarities in performance between our twin-cylinder configuration and a single bottom-referenced cylinder.

Acknowledgements

This research was supported by the Israel Science Foundation (Grant 464/13).

Appendix A. Comparison with previous results

In what follows, the results of using our methodology (as described in Section 3) are compared with published results by Garnaud and Mei (2010), Zheng et al. (2005), and Berggren and Johansson (1992).

Appendix A.1. Comparison with single-cylinder results

In the limit of large cylinder spacing, $H_2 \gg H_1$, the lower cylinder will be expected to have only negligible effects on the motion of the upper cylinder. Taking $R = H_1 = H_3 = 1.7$ m and water depth $h = 10$ m, with $H_2 = 6$ m reproduces the geometry considered in (Garnaud and Mei, 2010), where only a single cylinder was employed. The comparison of capture width and the (upper) cylinder's displacement is given in Figure A.1

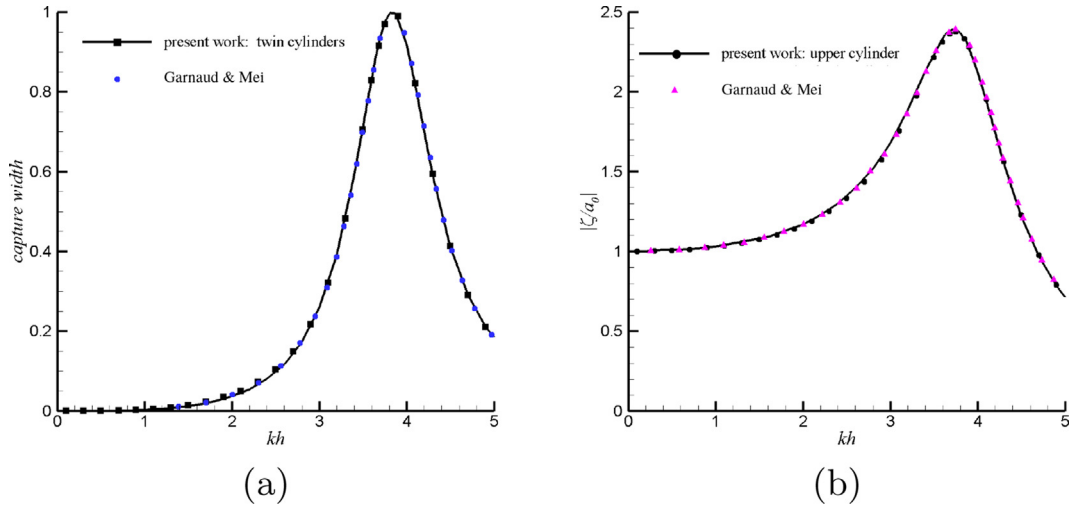

Fig. A.1. Comparison with Fig. 2 of (Garnaud and Mei, 2010) where $R = H_1 = H_3 = 1.7$ m, $H_2 = 6$ m, and $h = 10$ m. (a) Capture width. (b) Displacement of the upper cylinder.

Appendix A.2. Comparison with twin-cylinder results

Considering deep water, and restricting the motion to heave only allows a comparison with the work of Zheng et al. (2005) in Figure A.2 and Berggren & Johansson (Berggren and Johansson, 1992) in Figure A.3, which also demonstrates very good agreement.

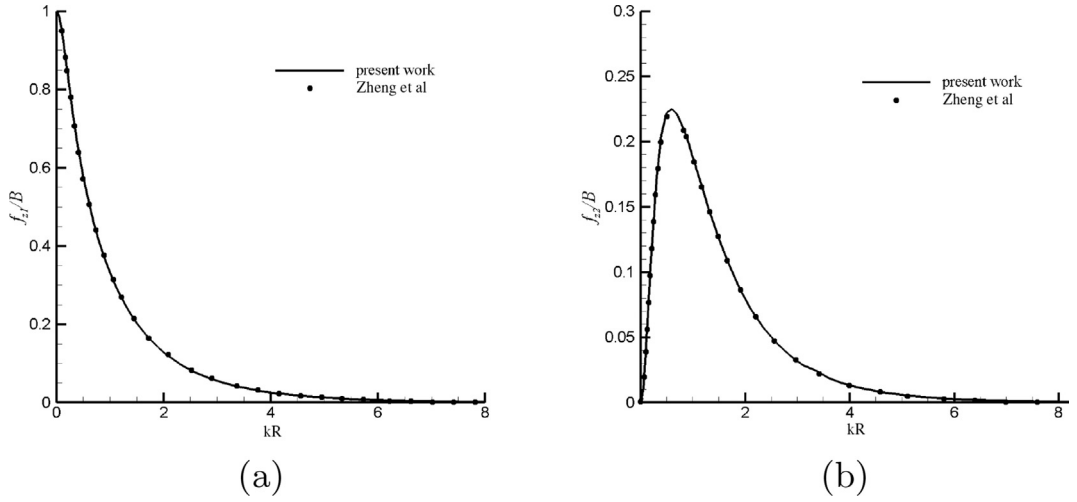

Fig. A.2. Comparison with Fig. 2 (a),(b) of Zheng et al. (2005), where $B = \rho g a_0 \pi R^2$, $h = 200$m, $R = 40$m, $H_1 = H_3 = 20$m, $H_2 = 30$m. (a) Exciting force f_{z1}/B on upper cylinder. (b) Exciting force f_{z2}/B on lower cylinder.

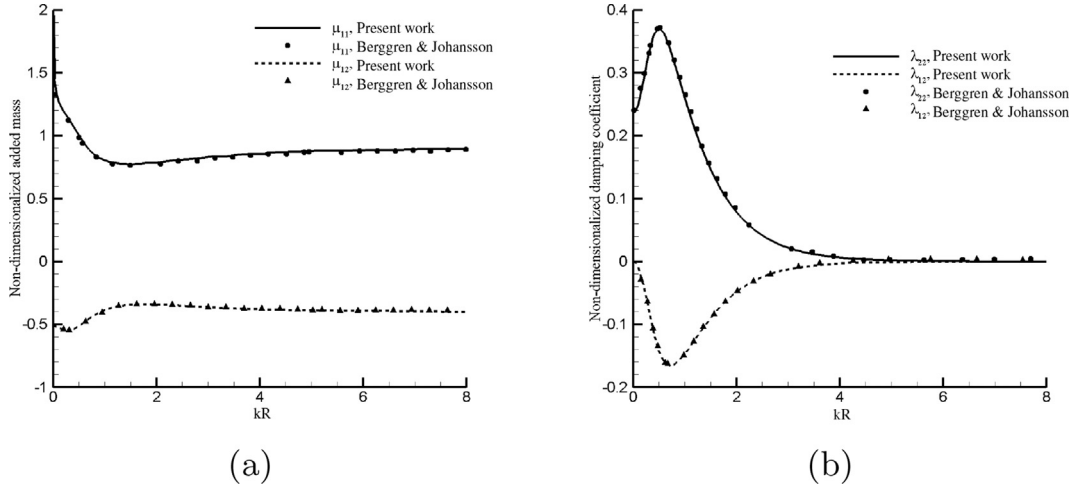

Fig. A.3. Comparison with Fig. 4 (a),(b) ($h_2/h_1 = 0.15$) of (Berggren and Johansson, 1992), $h = 200$m, $R = 40$m, $H_1 = H_3 = 20$m, $H_2 = 30$m. (a) Dimensionless added masses μ_{11}, μ_{12} for the upper cylinder. (b) Damping coefficients λ_{22}, λ_{12} for the upper cylinder.

References

Akrish, G., Schwartz, R., Rabinovitch, O., Agnon, Y., 2016. Impact of extreme waves on a vertical wall. Nat. Hazards 84 (2), 637–653.

Berggren, L., Johansson, M., 1992. Hydrodynamic coefficients of a wave energy device consisting of a buoy and a submerged plate. Appl. Ocean Res. 14 (1), 51–58.

Bhatta, D.D., 2007. Computation of added mass and damping coefficients due to a heaving cylinder. J. Appl. Math. Comput. 23 (1–2), 127–140.

Bhatta, D.D., 2011. Computations of hydrodynamic coefficients, displacement-amplitude ratios and forces for a floating cylinder due to wave diffraction and radiation. Int. J. Non-Linear Mech. 46 (8), 1027–1041.

Black, J.L., Mei, C.C., 1970. Scattering and Radiation of Water Waves. Tech. rep. no. 121. MIT Water Resources and Hydrodynamics Lab, Cambridge.

Black, J.L., Mei, C.C., Bray, M.C.G., 1971. Radiation and scattering of water waves by rigid bodies. J. Fluid Mech. 46 (1), 151–164.

Bódai, T., Srinil, N., 2015. Performance analysis and optimization of a box-hull wave energy converter concept. Renew. Energy 81, 551–565.

Borgarino, B., Babarit, A., Ferrant, P., 2012. Impact of wave interactions effects on energy absorption in large arrays of wave energy converters. Ocean. Eng. 41, 79–88.

Brown, A., Paasch, R., Tumer, I.Y., Lenee-Bluhm, P., Hovland, J., von Jouanne, A., Brekken, T., 2010. Towards a definition and metric for the survivability of ocean wave energy converters. In: ASME 2010 4th International Conference on Energy Sustainability, American Society of Mechanical Engineers, pp. 917–927.

Cerveira, F., Fonseca, N., Pascoal, R., 2013. Mooring system influence on the efficiency of wave energy converters. Int. J. Mar. Energy 3–4, 65–81.

Child, B.F.M., Venugopal, V., 2010. Optimal configurations of wave energy device arrays. Ocean. Eng. 37 (16), 1402–1417.

Coe, R.G., Neary, V.S., 2014. Review of methods for modeling wave energy converter survival in extreme sea states. In: Proceedings of the 2nd Marine Energy Technology Symposium (METS2014), Seattle, WA.

Crowe, C.T., Roberson, J.A., Elger, D.F., 2001. Engineering Fluid Mechanics. John Wiley & Sons.

Cummins, C.P., Dias, F., 2017. A new model of viscous dissipation for an oscillating wave surge converter. J. Eng. Math. 103 (1), 195–216.

Dean, R.G., Ursell, F., 1959. Interaction of a Fixed Semi-immersed Circular Cylinder with a Train of Surface Waves. Tech. rep.. MIT Hydrodynamics Laboratory. Tech. Rep. no. 37.

Engström, J., Eriksson, M., Isberg, J., Leijon, M., 2009. Wave energy converter with enhanced amplitude response at frequencies coinciding with Swedish west coast sea states by use of a supplementary submerged body. J. Appl. Phys. 106 (6).

Finnegan, W., Meere, M., Goggins, J., 2013. The wave excitation forces on a truncated vertical cylinder in water of infinite depth. J. Fluids Struct. 40, 201–213.

Fitzgerald, C.J., Thomas, G., 2007. A preliminary study on the optimal formation of an array of wave power devices. In: Proceedings of the 7th European Wave and Tidal Energy Conference.

Garnaud, X., Mei, C.C., 2010. Comparison of wave power extraction by a compact array of small buoys and by a large buoy. IET Renew. Power Gener. 4 (6), 519–530.

Garrett, C.J.R., 1971. Wave forces on a circular dock. J. Fluid Mech. 46, 129–139.

Göteman, M., Engström, J., Eriksson, M., Hann, M., Ransley, E., Greaves, D., Leijon, M., 2015. Wave loads on a point-absorbing wave energy device in extreme waves. J. Ocean Wind Energy 2 (3), 944–950.

Hong, Y., Waters, R., Boström, C., Eriksson, M., Engström, J., Leijon, M., 2014. Review on electrical control strategies for wave energy converting systems. Renew. Sustain. Energy Rev. 31, 329–342.

Kroszynski, U.I., Stiassnie, M., 1979. Wave power estimates on Eastern Mediterranean coast. J. Energy Div. ASCE 105 (EY1) 159–164.

Linton, C.M., McIver, P., 2001. Handbook of Mathematical Techniques for Wave/structure Interactions. CRC Press.

Maisondieu, C., 2015. WEC survivability threshold and extractable wave power. In: Proceedings of the 11th European Wave and Tidal Energy Conference.

McGuinness, J., Thomas, G., 2015. Optimal arrangements of elementary arrays of wave power devices. In: Proceedings of the 11th European Wave and Tidal Energy Conference.

McGuinness, J.P., Thomas, G., 2016. Hydrodynamic optimisation of small arrays of heaving point absorbers. J. Ocean Eng. Mar. Energy 2 (4), 439–457.

Miles, J., Gilbert, F., 1968. Scattering of gravity waves by a circular dock. J. Fluid Mech. 34, 783–793.

Stallard, T.J., Weller, S.D., Stansby, P.K., 2009. Limiting heave response of a wave energy device by draft adjustment with upper surface immersion. Appl. Ocean Res. 31 (4), 282–289.

Stiassnie, M., Kadri, U., Stuhlmeier, R., 2016. Harnessing wave power in open seas. J. Ocean Eng. Mar. Energy 2 (1), 47–57.

Teillant, B., Costello, R., Weber, J., Ringwood, J., 2012. Productivity and economic assessment of wave energy projects through operational simulations. Renew. Energy 48, 220–230.

Ursell, F., 1949. On the heaving motion of a circular cylinder on the surface of a fluid, Quart. J. Mech. Appl. Math. 2, 218–231.

Wu, B., Wang, X., Diao, X., Peng, W., Zhang, Y., 2014. Response and conversion efficiency of two degrees of freedom wave energy device. Ocean. Eng. 76, 10–20.

Yeung, R.W., 1981. Added mass and damping of a vertical cylinder in finite-depth waters. Appl. Ocean Res. 3 (3), 119–133.

Zheng, Y.H., Shen, Y.M., You, Y.G., Wu, B.J., Rong, L., 2005. Hydrodynamic properties of two vertical truncated cylinders in waves. Ocean. Eng. 32 (3–4), 241–271.